



OPEN ACCESS

EDITED AND REVIEWED BY
Costanza Bonadiman,
University of Ferrara, Italy

*CORRESPONDENCE
Luca Toffolo,
✉ luca.toffolo@unimi.it

[†]PRESENT ADDRESS
Francesca Miozzi,
Earth and Planets Laboratory, Carnegie
Institution for Science, Washington, DC,
United States

RECEIVED 30 June 2023
ACCEPTED 11 July 2023
PUBLISHED 26 July 2023

CITATION

Toffolo L, Tumiatì S, Villa A, Fumagalli P,
Amalfa A and Miozzi F (2023),
Corrigendum: Experimental dissolution
of carbonaceous materials in water at
1 GPa and 550°C: assessing the role of
carbon forms and redox state on COH
fluid production and composition during
forearc subduction of organic matter.
Front. Earth Sci. 11:1250573.
doi: 10.3389/feart.2023.1250573

COPYRIGHT

© 2023 Toffolo, Tumiatì, Villa, Fumagalli,
Amalfa and Miozzi. This is an open-access
article distributed under the terms of the
[Creative Commons Attribution License
\(CC BY\)](https://creativecommons.org/licenses/by/4.0/). The use, distribution or
reproduction in other forums is
permitted, provided the original author(s)
and the copyright owner(s) are credited
and that the original publication in this
journal is cited, in accordance with
accepted academic practice. No use,
distribution or reproduction is permitted
which does not comply with these terms.

Corrigendum: Experimental dissolution of carbonaceous materials in water at 1 GPa and 550°C: assessing the role of carbon forms and redox state on COH fluid production and composition during forearc subduction of organic matter

Luca Toffolo^{1*}, Simone Tumiatì¹, Alberto Villa²,
Patrizia Fumagalli¹, Andrea Amalfa¹ and Francesca Miozzi^{1†}

¹Dipartimento di Scienze della Terra "Ardito Desio", University of Milan, Milan, Italy, ²Dipartimento di Chimica, University of Milan, Milan, Italy

KEYWORDS

carbonaceous matter, graphite, subduction, experimental petrology, COH fluids, dissolution

A Corrigendum on

[Experimental dissolution of carbonaceous materials in water at 1 GPa and 550°C: assessing the role of carbon forms and redox state on COH fluid production and composition during forearc subduction of organic matter](#)

by Toffolo L, Tumiatì S, Villa A, Fumagalli P, Amalfa A and Miozzi F (2023). *Front. Earth Sci.* 11: 1013014. doi: 10.3389/feart.2023.1013014

In the published article, there was an error in [Table 4](#); [Figure 6](#) as published.

[Table 4](#) contains a formatting error where C(sp^2) was incorrectly assigned to the survey XPS analysis, when in fact it belongs to the C 1s spectra. Additionally, the carbon in C=O and O=C-OH groups was mistakenly classified as sp^3 , whereas it is actually sp^2 -hybridized.

In [Figure 6](#), there is an error where OFGs (oxygen functional groups) were mistakenly grouped together with carbon in C-C bonds as sp^3 species. In the updated version of the figure, the lower vertexes are now labeled as OFGs and C(sp^3), grouping all the OFGs regardless of their carbon hybridization and specifically identifying sp^3 -hybridized carbon in carbon-carbon bonds, respectively. The caption has also been modified accordingly to reflect these corrections.

The corrected [Table 4](#); [Figure 6](#) and their captions appear below.

In the published article, there was an error. All the carbon atoms in the oxygenated functional groups detected by XPS were incorrectly labeled as sp^3 -hybridized, whereas carbon possesses this hybridization solely in the C-O group. Though minor, this error has

TABLE 4 Results of XPS analyses.

	Survey		C 1s				
	C 1s	O 1s	$C(sp^2)$			$C(sp^3)$	
			C–C ^a	C=O	O=C–OH	C–C	C–O
Graphite							
B.E. (eV)	284.2	531.2	284.4	287.5	—	—	285.8
A.P. (%)	99.4	0.6	99.4	0.5	—	—	0.1
Graphite oxide							
B.E. (eV)	284.1	531.1	284.3	290.4	—	285.2	287.4
A.P. (%)	69.2	30.8	1.7	6.8	—	57.1	34.4
Mesoporous carbon							
B.E. (eV)	284.1	531.1	284.8	—	—	—	—
A.P. (%)	99.6	0.4	93.3	0.8	0.4	4.6	0.9
Vulcan[®] carbon							
B.E. (eV)	284.5	531.5	284.4	287.1	288.8	—	285.7
A.P. (%)	99	1	70.5	8	3.8	—	17.7
Glass-like carbon							
B.E. (eV)	284.3	532	284.5	287.4	288.4	285.3	285.9
A.P. (%)	92.4	7.6	87.5	3	0.8	2.4	6.3
COH203 (char from microalgae pyrolysis at 1 GPa, 550°C)							
B.E. (eV)	284.6	532.2	284.6	287.3	—	285.3	286.2
A.P. (%)	68.7	15.1	51.1	11	—	21	16.9
DOL (kerogen, ~100°C)							
B.E. (eV)	284.6	532.1	284.5	287.9	289.1	285.6	286.3
A.P. (%)	80.2	19.8	33.2	9.1	0.6	38.2	18.9
TAV-M938 (CM, ~350°C, 0.6–1 GPa)							
B.E. (eV)	n.d.	n.d.	284.4	287.6	288.8	285.6	286.7
A.P. (%)	n.d.	n.d.	80.5	3.1	0.7	8.3	7.4

^aC–C in this column indicates a generic bond between carbon atoms, which can exist as either a single or a double covalent bond.

B.E., binding energy; A.P., atomic percentage; n.d., not determined.

been repeated multiple times throughout the manuscript. A correction has been made to the **Abstract**. The updated **Abstract** appears below:

“Biogenic carbonaceous material (CM) is the main carrier of organic carbon in the subduction zone and contributes to COH fluid production and volcanic arc gaseous emissions. Here we investigated the effect of the structural, textural and chemical heterogeneity of CM on its reactivity and redox dissolution by conducting short-lived (1 h) experiments, where synthetic analogues of CM [ordered graphite, graphite oxide (GO), mesoporous carbon (MC), Vulcan[®] carbon (VC) and glass-like carbon (GC)], are reacted with water at $p = 1$ GPa and $T = 550^\circ\text{C}$ —conditions typical of a warm forearc subduction—and $f\text{O}_2$ buffered from $\Delta\text{FMQ} \approx +4$ to -7 . We show that the amount of

dissolved CM ($\text{CM}_{\text{dissolved}}$) and the proportion of volatile carbon species ($\text{C}_{\text{volatile}}$) in the fluid is related both to the structure and the peculiar surficial properties of the carbon forms, such as carbon sp^2 - and sp^3 -hybridization, amount of oxygen heteroatoms, presence of oxygenated functional groups (OFGs) and of active sites. MC and graphite ($\text{C}(sp^2) > 94$ at%, $\text{O} < 1$ at%, OFGs < 2.2 at %, high proportion of active sites) are relatively inert ($\text{CM}_{\text{dissolved}} < 0.4$ mol%) but the former reacts more extensively at extreme redox conditions (producing $\text{CO}_2 + \text{CO}$ and $\text{CO}_2 + \text{CH}_4$ $\text{C}_{\text{volatile}}$ mixtures at $\Delta\text{FMQ} \approx +4$ and -7 , respectively), while the latter has a maximum of $\text{C}_{\text{volatile}}$ production ($\text{CO}_2 + \text{CH}_4$) at $\Delta\text{FMQ} \approx 0$, which is not observed in a 10-day long run; partly-ordered GO ($\text{C}(sp^3) \sim 92$ at%, $\text{O} \sim 31$ at%, OFGs ~ 41 at%) is the most reactive material at all redox conditions ($\text{CM}_{\text{dissolved}} > 2.6$ mol%) and

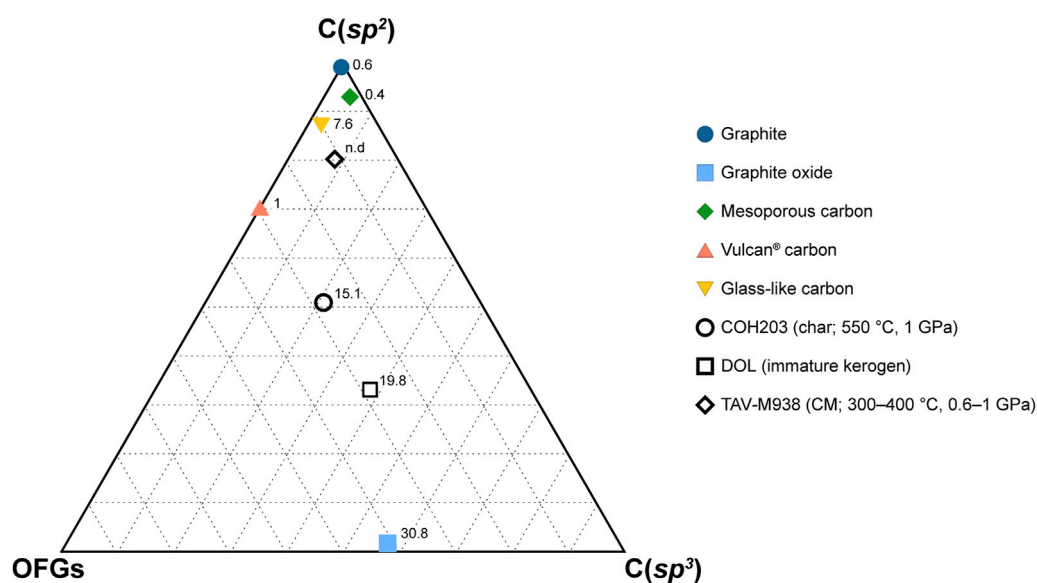


FIGURE 6

Ternary diagram reporting XPS C 1s composition of both synthetic and natural carbonaceous materials. The vertices labeled $C(sp^2)$ and $C(sp^3)$ indicate sp^2 - and sp^3 -hybridized carbon in carbon-carbon bonds only. The OFGs vertex represents the overall proportion of oxygenated functional groups, regardless of carbon hybridization. The numbers accompanying the markers indicate the oxygen content (in at%) obtained from XPS survey analysis. The data utilized for constructing the figure can be found in Table 4.

produces CO_2 as the dominant C_{volatile} species; disordered GC, and VC ($C(sp^3) < 18$ at%, O < 8 at%, OFGs < 30 at%) are more reactive at $\Delta FMQ \approx +4$ ($CM_{\text{dissolved}} \sim 1$ mol%) and $\Delta FMQ \approx -7$ ($CM_{\text{dissolved}} > 1$ mol%), where C_{volatile} is dominantly CO_2 and CH_4 , respectively. Besides the significant deviations from thermodynamically predicted graphite-saturated COH fluid composition and speciation, our results suggests that: 1) immature CM [disordered, rich in $C(sp^3)$, O, OFGs] is preferentially dissolved under high fluid fluxes and may buffer fluids to rather oxidizing conditions; 2) a descending flux of oxygen (and hydrogen) bond to CM may exist.”

A correction has been made to Section 2.3.3 “XPS.” The updated text appears below:

“The deconvolution of HR C 1s spectra allows to evaluate the relative concentration of sp^2 - and sp^3 -hybridized carbon species. These species can be found in carbon-carbon bonds (with average binding energies, B.E., of ~ 284.5 V and ~ 285.4 eV for $C(sp^2)$ and $C(sp^3)$, respectively) and in carbon-oxygen bonds, forming oxygenated functional groups (C–O, C=O, O=C–OH; represented by components at B.E ≥ 285.7 eV).”

A correction has been made to Section 4.1 “Reactivity of carbon forms.” The updated text appears below:

“[...] GO is the most reactive carbon form, in that it shows the highest values of $CM_{\text{dissolved}} (>2\%)$, and produces fluids in which the dominant volatile carbon species is always CO_2 . This behavior can be ascribed to its very high proportion of both $C(sp^3)$ (~ 92 at%) and O heteroatoms (>30 at%; Table 4). It has been shown that by heating GO oxygenated functional groups—i.e., epoxy (C–O–C), carbonyl (C=O), hydroxide (C–OH)—in part decompose and react with carbon to give a gas composed of H_2O , CO, CH_4 and CO_2 (da Silva et al., 2018; He et al., 1998; Zhang et al., 2018) and in part

reorganize (hydroxyl and epoxy groups decrease, while carbonyl and cyclic ether groups increase; da Silva et al., 2018) [...]”

Corrections have been made to Section 4.2 “Synthetic carbon forms as compositional endmembers of natural CM.” The changes appear below:

“Kerogen from DOL is closer to GO endmember, having a comparable oxygen concentration (~ 20 at% and ~ 31 at%, respectively) and a relatively high content of $C(sp^3)$ in carbon-carbon bonds (~ 36 at% vs. ~ 57 at%) and of oxygenated functional groups ($\sim 29\%$ vs. $\sim 41\%$). Immature CM, in fact, is rich in oxygen (generally the atomic O/C ratios are comprised between 0.03 and 0.3) and in $C(sp^3)$, related to a high proportion of oxygenated functional groups and of aliphatic molecules (Vandenbroucke and Largeau, 2007). Along with the temperature increase that accompanies sediment lithification and metamorphism, CM loses oxygen and develops a more aromatic character, i.e., the proportion of $C(sp^2)$ increases, and organizes into a more ordered structure (e.g., Buseck and Huang, 1985; Vandenbroucke and Largeau, 2007; Buseck and Beyssac, 2014). However, the gain in aromaticity of CM not necessarily leads to a perfectly ordered structure (i.e., graphite), which require further polymerization and structural reorganization (Buseck and Huang, 1985; Buseck and Beyssac, 2014). This is clear in the natural CM sample TAV-M938, which mainly contains sp^2 -hybridized carbon-carbon bonds (~ 81 at%) but it is structurally disordered, being composed of a mixture of diffraction-amorphous microporous and mesoporous textures, the latter being the result of low to moderate grades of metamorphism (Buseck and Huang, 1985; Beyssac et al., 2002b).”

Corrections have been made to Appendix A. The updated Appendix appears below.

The five synthetic carbon forms are characterized by distinct microtextures, crystallinity, carbon hybridization, content of oxygen heteroatoms and type of oxygenated functional groups, as described below (cf. Table 4).

Graphite (**Supplementary Figure S2A**) forms aggregates of ~5 nm-thick sub-circular platelets that have diameter of few to several tens of nanometers and in cross section have a layered structure. It is perfectly crystalline, as shown by the presence of hkl reflections in the SAED pattern. The Raman spectrum is dominated by a sharp and intense G peak at ~1,574 cm^{-1} ; D peak at 1,345 cm^{-1} is broad and weak. Graphite is almost pure sp^2 -hybridized carbon ($\text{O} < 1 \text{ at}\%$).

Graphite oxide (GO) (**Figure 2A**) is composed of sheets with a thickness up to a few tenths of nanometers that locally show a layered organization, i.e., the presence of some large (up to ~10 nm) crystalline domains. This partial ordering is indicated by the presence of modulations of the diffraction bands in the SAED pattern (**Beyssac et al., 2002b**). Its Raman spectrum shows two similarly intense D and G peaks, at ~1,354 cm^{-1} and ~1,605 cm^{-1} , respectively. GO has the highest concentration of sp^3 -hybridized carbon (~92 at%) and oxygen heteroatoms (~31 at%). In GO there is a large proportion of oxygenated functional groups (~41 at%).

Mesoporous carbon (MC) (**Figure 2B**) is made of ~5 nm thick carbon layers wrapped into polygonal shapes, which enclose pores with a diameter comprised between few nanometers and 15–20 nm. The SAED patterns show sharp and intense diffraction bands. Its Raman spectrum is characterized by D and G positioned at ~1,340 cm^{-1} and ~1,576 cm^{-1} , respectively, with the former being more intense than the latter. MC is nearly pure carbon ($\text{O} < 1 \text{ at}\%$), composed of dominant sp^2 -hybridized carbon (~95 at%); it has a small proportion of C(sp^3) mainly related to C–C bonds (~5 at%).

Vulcan® carbon (VC) (**Figure 2C**) is composed of rounded particles with a diameter of ~50 nm and a vague concentric layered structure. The low degree of structural organization is denoted by the presence of wide and weak diffraction bands in SAED patterns. Its Raman spectrum shows broad and similarly intense D and G peaks at ~1,356 cm^{-1} and ~1,588 cm^{-1} , respectively. VC exhibits a notable proportion of sp^3 -hybridized carbon (~18 at%), which is entirely due to the presence of oxygenated functional groups. A substantial amount of oxygenated functional groups is present (~30 at%).

Glass-like carbon (GC) (**Supplementary Figure S2B**) consists of a nanometer-scale tangle of graphitic sheets (cf. **Shiell et al., 2018**). As a consequence of this low degree of atomic organization, the related SAED pattern shows very faint and broad diffraction bands, indistinguishable from that of the holey amorphous carbon support

grid. In the Raman spectrum D and G peaks, positioned at ~1,354 cm^{-1} and ~1,602 cm^{-1} , respectively, are both broad, but the former is more intense than the latter. GC contains a small proportion of oxygen heteroatoms (~8 at%) and it is principally composed of sp^2 -hybridized carbon (~91 at%). Notably, oxygenated functional groups constitute a significant percentage (~10 at%).

Char was produced from the pyrolysis at 550°C and 1 GPa of green microalgae (experiment COH203). Char is disordered—the Raman spectrum shows a broad D peak at ~1,344 cm^{-1} and a more intense and narrower G peak at ~1,600 cm^{-1} —, but locally some small hexagonal graphite crystals (diameter $\leq 300 \mu\text{m}$) can be found (**Figure 7B**). The char surface has a moderate proportion of oxygen heteroatoms (~18 at%) and an high content of both sp^2 - and sp^3 -hybridized carbon species (~62 at% and ~38 at%, respectively); it also contains a significant amount of oxygenated functional groups (~28 at%).

Kerogen extracted from natural sample DOL has a Raman spectrum characterized by high background fluorescence from which a broad D peak at ~1,350 cm^{-1} and a quite sharp G peak at ~1,579 cm^{-1} emerge (**Supplementary Figure S4**). Kerogen has a high content of oxygen heteroatoms (~20 at%) and a large proportion of sp^3 -hybridized carbon (~57 at%); additionally, it contains a considerable amount of oxygenated functional groups (~29 at%).

Carbonaceous material separated from natural sample TAV-M938 (**Figure 7A**) is structurally and texturally heterogeneous at a $< 1 \mu\text{m}$ scale: it is mainly disordered material, characterized by both concentric layered and mesoporous textures, but locally exhibits ordered graphite-like portions. The Raman spectrum shows a broad and intense D peak at ~1,350 cm^{-1} and narrower and less intense G peak at 1,604 cm^{-1} . Carbonaceous material has a high proportion of sp^2 -hybridized carbon (~84 at%) and a significant overall amount of oxygenated functional groups (~11 at%).

The authors apologize for these errors and state that this does not change the scientific conclusions of the article in any way. The original article has been updated.

Publisher's note

All claims expressed in this article are solely those of the authors and do not necessarily represent those of their affiliated organizations, or those of the publisher, the editors and the reviewers. Any product that may be evaluated in this article, or claim that may be made by its manufacturer, is not guaranteed or endorsed by the publisher.